Mathematical Model of Mass Transport through Dispersed-Phase Polymer Networks

Charalambos G. Varelas and David G. Dixon
Dept. of Chemical and Metallurgical Engineering, Mackay School of Mines, University of Nevada, Reno, NV 89557

Carol A. Steiner
Dept. of Chemical Engineering, The City College of CUNY, New York, NY 10031

A mathematical model of mass transport through dispersed-phase networks to be used for the sustained release of drugs or other solutes at steady rates is presented. The drug is assumed to be encapsulated within the dispersed microdomains and transported to the bulk by diffusion across the interface. A drug is released to the surroundings by diffusion through the bulk. The results show that the desired steady flux of a drug to the surroundings may be obtained given appropriate values of structural properties of the network. These properties may be manipulated easily in the fabrication of dispersed-phase networks reported previously.

Introduction

Zero-order release, or the release of a solute or drug from a substrate to the surroundings at a steady rate over long periods, is a much sought after property for controlled-release devices and certain types of chemical reactors. Clearly, simple diffusion from a monolithic device will yield a concentration-dependent release profile. This problem can be overcome by coupling two or more rate processes in a single device. Many workers in recent years have conceived a host of devices based on this strategy, including reservoir devices such as the commercial skin patches, hydrogels with swelling fronts, multilayered tablets, and others (for example, Baker, 1987). All of these devices have inherent disadvantages, however, and research in this field continues apace.

One approach to obtaining zero-order release is through a dispersed-phase network in which the dispersed phase, or microdomains, can serve as reservoirs for solutes or drugs permeating the network. The bulk phase serves as a diffusion pathway from the microdomains to the surroundings. The drug enters the bulk phase from the reservoirs by diffusion across the interface, and is released to the surroundings by diffusion through the bulk to the surface of the device. While both of these fluxes are time-dependent, if they can be made to match initially then for some finite period at least the concentration of drug in the bulk phase will exhibit a pseudo-steady state and zero-order release to the surroundings can be achieved.

Our group has fabricated dispersed-phase hydrogels characterized by hydrophobic microdomains in a water-swollen polymer network. We have learned to manipulate their struc-

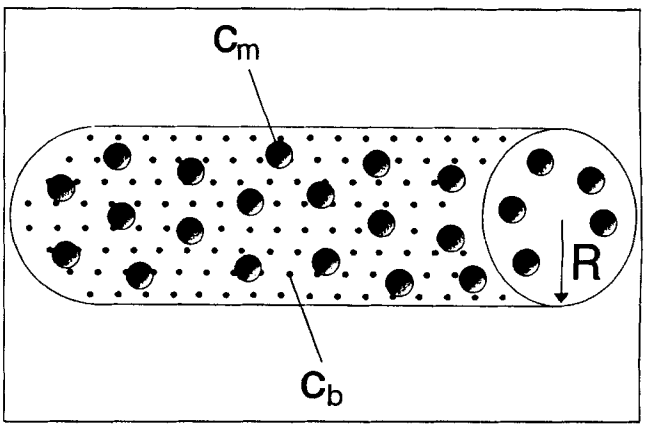

Figure 1. Cylindrical, dispersed-phase, controlled-release device.
It shows microdomains and bulk phase both saturated with drug.

Present address of D. G. Dixon: Dept. of Metals and Materials Engineering, University of British Columbia, Vancouver, BC, V6T 1Z4 Canada.

ture (Dualeh and Steiner, 1991, 1992; Varelas and Steiner, 1992; Wu et al., 1995) and have also obtained some preliminary results demonstrating that a constant release rate of model drugs can be sustained for prolonged periods from these gels (Varelas et al., 1995). In this article we present a mathematical model of mass transfer through dispersed-phase materials with drug encapsulated in the microdomains. The model was developed to allow us to predict the optimum structure for a hydrogel to be used for the sustained release of a drug of known chemical structure and diffusivity through water. The predictions of the model may be used as the design basis for hydrogels tailored for the release of particular drugs.

Model Formulation

The purpose of this model is to analyze the release profile of solutes exiting a dispersed-phase network in which the dispersed phase acts as a reservoir. Our goal is to optimize the structure of the network such that a constant rate of release may be achieved for a particular drug over long periods. Thus the model should enable us to correlate the duration and rate of zero-order release with structural properties of the network and drug.

The device operates as follows (Figure 1). Initially, the material is impregnated with a drug or another solute such that the drug partitions preferentially into the dispersed phase, or microdomains. On exposure of the gel to drug-free surroundings, the drug exits the gel from the bulk phase in accordance with Fick's law. The drug is simultaneously restored to the bulk phase from the microdomains. The gel properties that influence the mass-transfer rates are the total interfacial area of the microdomains, A_i, and the mass-transfer resistance of the microdomain/bulk interface, h_i. The important solute properties are the partition coefficient, α, of the solute between the two phases of the gel (which also depends on the gel structure) and the diffusion coefficient of the solute in the bulk phase, D_b. In addition, the total drug loading in the device will depend on α and the volume fraction of microdomains, ϕ.

The continuity equation for this system is given by

$$\frac{\partial \bar{c}}{\partial t} = D_{\text{eff}} \nabla^2 \bar{c} \tag{1}$$

where

$$\bar{c} = (1-\phi)c_b + \phi c_m \tag{2}$$

and

$$D_{\text{eff}} = (1+3\phi)D_b. \tag{3}$$

Equation 3 comes from the Maxwell relation regarding mass transfer through a dispersion in which diffusion through the dispersed particles is extremely rapid (Cussler, 1984). This assumption also allows us to neglect the concentration gradient inside the microdomains, so Eq. 1 becomes

$$(1-\phi)\frac{\partial c_b}{\partial t} = (1-\phi)D_{\text{eff}}\nabla^2 c_b - \phi\frac{\partial c_m}{\partial t}. \tag{4}$$

Equation 4 describes the unsteady-state flux of drug in the bulk phase, with Fick's law governing diffusion out of the bulk and a source term giving the rate of input of drug to the bulk from the microdomains. The form of the source term will depend on the mechanism for interfacial mass transfer. We assume that the microdomains behave as well-stirred reservoirs containing drug that crosses the interface according to first-order kinetics, as follows:

$$\phi\frac{\partial c_m}{\partial t} = -\frac{hA_i}{V}(\alpha c_m - c_b). \tag{5}$$

The boundary and initial conditions for this system are given by

$$\begin{aligned} c_b(r,t=0) &= c^* \\ c_b(r=R,t) &= 0 \\ \frac{\partial c_b}{\partial r}(r=0,t) &= 0 \\ c_m(r,t=0) &= \frac{c^*}{\alpha}. \end{aligned} \tag{6}$$

The device is assumed to be a section of an infinitely long cylinder immersed in a drug-free solution that is rapidly and continuously flowing past the surface of the device. The partition coefficient, α, gives a measure of the maximum driving force for interfacial mass transfer, and the ratio of h to D_b is a measure of the relative rates of mass transfer to and through the bulk phase.

The parameter h represents the overall mass-transfer resistance at the interface, including contributions from the microdomain/bulk interface itself (h_i) and any stagnant boundary layer of solute that forms around the microdomains (h_b). Thus h can be evaluated by adding the reciprocals of the resistances h_i and h_b, with h_b (coming from the Sherwood number analysis for spherical particles in the absence of flow) given by $h_b = D_b/r_m$, where r_m is the radius of the microdomains. This gives

$$\frac{1}{h} = \frac{1}{h_i} + \frac{r_m}{D_b}, \tag{7}$$

which approaches $1/h_i$ as $r_m \to 0$. This expression demonstrates the dependence of h on D_b. Note that by expressing the interfacial mass-transfer resistance in terms of the composite parameter h we have generalized the equations to any microdomain geometry.

Nondimensionalizing the model equations allows us to analyze the important design parameters. We introduce the following dimensionless variables and parameters:

$$\tilde{c}_b = \frac{c_b}{c^*} \qquad \tilde{c}_m = \frac{\alpha c_m}{c^*} \qquad \tilde{r} = \frac{r}{R} \qquad \tau = \frac{D_{\text{eff}}t}{R^2}$$

$$\tilde{\nabla}^2 = R^2\nabla^2 \qquad \lambda = \frac{hA_iR^2}{(1-\phi)VD_{\text{eff}}} \qquad \kappa = \frac{\alpha(1-\phi)}{\phi}. \tag{8}$$

Then Eqs. 4 and 5 become

$$\frac{\partial \tilde{c}_b}{\partial \tau} = \tilde{\nabla}^2 \tilde{c}_b - \frac{1}{\kappa}\frac{\partial \tilde{c}_m}{\partial \tau} \tag{9}$$

$$\frac{\partial \tilde{c}_m}{\partial \tau} = -\kappa\lambda(\tilde{c}_m - \tilde{c}_b) \tag{10}$$

with dimensionless boundary and initial conditions

$$\tilde{c}_b(\tilde{r},\tau = 0) = 1$$

$$\tilde{c}_b(\tilde{r} = 1,\tau) = 0$$

$$\frac{\partial \tilde{c}_b}{\partial \tilde{r}}(\tilde{r} = 0,\tau) = 0$$

$$\tilde{c}_m(\tilde{r},\tau = 0) = 1. \tag{11}$$

The parameter κ is a distribution coefficient, defined such that a low κ corresponds to a high proportion of drug in the microdomains at time zero. Thus for constant h and D_{eff}, the lower the value of κ the longer the period during which a finite flux is observed at the surface of the device. The parameter λ is the Damköhler number (Rosner, 1986), giving the ratio of the characteristic times for diffusion through the bulk and introduction of solute into the bulk from the dispersed phase. A zero λ is the case with no active microdomains; λ very high would result in rapid depletion of the microdomains, giving a vanishingly short time for zero-order release. An intermediate value of λ coupled with a low value of κ will produce sustained release of the drug at a rate that decays very slowly over time—in effect, a zero-order release plateau. Note that for the case of spherical microdomains surrounded by a boundary layer λ becomes $\lambda = h_i A_i R^2/[(1-\phi)V(D_{\text{eff}} + (1+3\phi)h_i r_m)]$.

Solution of the Model

Equations 9 and 10 are solved simultaneously by means of Laplace transforms (Churchill, 1958) that take the form

$$s\bar{c}_b - 1 = \tilde{\nabla}^2 \bar{c}_b - \frac{1}{\kappa}(s\bar{c}_m - 1) \tag{12}$$

$$s\bar{c}_m - 1 = -\kappa\lambda(\bar{c}_m - \bar{c}_b) \tag{13}$$

where s is the Laplace domain variable, and the overbar denotes transformed variables (that is, functions of s). Solving Eq. 13 for $\bar{c}_m$ and substituting into Eq. 12 gives

$$\tilde{\nabla}^2 \bar{c}_b - M^2(s)\bar{c}_b = -\frac{M^2(s)}{s} \tag{14}$$

where $M(s)$ is defined

$$M(s) = \left[s + \frac{s\lambda}{s+\kappa\lambda}\right]^{1/2}. \tag{15}$$

Equation 14 has the boundary conditions

$$\bar{c}_b(\tilde{r} = 1,s) = 0$$

$$\frac{\partial \bar{c}_b}{\partial \tilde{r}}(\tilde{r} = 0,s) = 0. \tag{16}$$

The homogeneous part of Eq. 14 is the modified zero-order Bessel function. The solution to Eqs. 14 through 16 in the Laplace domain is

$$\bar{c}_b = \frac{1}{s}\left(1 - \frac{I_0[M(s)\tilde{r}]}{I_0[M(s)]}\right). \tag{17}$$

Upon inversion from the Laplace domain one obtains the real-time solution for bulk solute concentration

$$\tilde{c}_b(\tilde{r},\tau) = -\sum_{k=1}^{2}\sum_{n=1}^{\infty}\frac{2\xi_n J_0(\xi_n\tilde{r})e^{s_k^n\tau}}{s_k^n J_1(\xi_n)N(s_k^n)} \tag{18}$$

where $N(s_k^n)$ is defined

$$N(s_k^n) = 1 + \frac{\kappa\lambda^2}{(s_k^n + \kappa\lambda)^2} \tag{19}$$

and ξ_n = zeros of the zero-order Bessel function of the first kind, J_0. Furthermore, the quadratic roots s_k^n are defined

$$s_k^n = s_{1,2}^n = \frac{-(\xi_n^2 + \lambda + \kappa\lambda) \pm \sqrt{(\xi_n^2 + \lambda + \kappa\lambda)^2 - 4\kappa\lambda\xi_n^2}}{2}. \tag{20}$$

A detailed description of the inversion procedure and the meanings of terms in Eq. 18 are given in the Appendix.

By application of Duhamel's theorem (Churchill, 1958), we obtain an expression for the solute concentration in the microdomains

$$\tilde{c}_m(\tilde{r},\tau) = e^{-\kappa\lambda\tau} + \kappa\lambda\int_0^\tau \tilde{c}_b(\tilde{r},\tau)e^{-\kappa\lambda(\tau-\tau')}d\tau'. \tag{21}$$

Substitution of Eq. 18 into Duhamel's integral and subsequent evaluation give

$$\tilde{c}_m(\tilde{r},\tau) = e^{-\kappa\lambda\tau} - \kappa\lambda\sum_{k=1}^{2}\sum_{n=1}^{\infty}\frac{2\xi_n J_0(\xi_n\tilde{r})(e^{s_k^n\tau} - e^{-\kappa\lambda\tau})}{s_k^n(s_k^n + \kappa\lambda)J_1(\xi_n)N(s_k^n)}. \tag{22}$$

Equation 18 and 22 can be solved to give the concentration profiles in the bulk and the microdomains as a function of radial position within the device. In addition, we can solve for the flux of solute from the surface of the device

$$\tilde{j}_b(\tilde{r} = 1,\tau) = -\left[\frac{\partial \tilde{c}_b}{\partial \tilde{r}}\right]_{\tilde{r}=1} = -\sum_{k=1}^{2}\sum_{n=1}^{\infty}\frac{2\xi_n^2 e^{s_k^n\tau}}{s_k^n N(s_k^n)} \tag{23}$$

where

$$\tilde{j}_b = \frac{j_b R}{D_{\text{eff}} c^*} \tag{24}$$

From this, the mass of solute released from the device as of time, M_τ, is given by

$$\frac{M_\tau}{M_\infty} = \frac{2\kappa}{\kappa+1}\int_0^\tau \tilde{j}_b(\tilde{r}=1,\tau)\,d\tau$$

$$= \frac{2\kappa}{\kappa+1}\sum_{k=1}^{2}\sum_{n=1}^{\infty}\frac{2\xi_n^2(1-e^{s_k^n\tau})}{(s_k^n)^2 N(s_k^n)} \tag{25}$$

expressed here as a fraction of M_∞, the mass of solute available for eventual release from the device. Equations 23 and 25 thus give the release profiles of the drug into the surroundings as a function of time. Their analysis will provide insight into the effects of the parameters κ and λ on the efficacy of a dispersed-phase hydrogel in service as a controlled-release device.

Results

Typical concentration profiles $\tilde{c}_b(\tilde{r})$ and $\tilde{c}_m(\tilde{r})$ obtained by solving Eqs. 18 and 22, respectively, are shown in Figures 2a–c for $\kappa = 0.1$ and $\lambda = 0.01$, 0.1, and 1.0. The time intervals $\bigcirc\tau$ are the same for the same diffusing species and microdomain content regardless of κ. Note the different vertical scales on each plot. These figures illustrate several important effects. First, the magnitude of the flux of the drug to the surroundings is given by the slope of the lower curve $\tilde{c}_b$ vs. $\tilde{r}$ at $\tilde{r} = 1$. Clearly, when $\lambda = 1$ (Figure 2c), the flux changes significantly with time. When $\lambda = 0.1$ and 0.01, there is an initial high transient flux, after which the $\tilde{c}_b$ vs. $\tilde{r}$ curves superimpose for at least four time intervals, giving a constant release rate. However, the magnitude of the flux during the constant release plateau is a strong function of λ, as expected. Where λ is very low (Figure 2a), slow release from the microdomains limits the bulk concentration of solute; consequently, the net flux to the surroundings is low. A more permeable interface (and hence a higher λ) releases the drug to the bulk more rapidly. This effect is illustrated by the upper row of profiles, $\tilde{c}_m$ vs. $\tilde{r}$, in Figures 2a–c. For λ very high (Figure 2c), the microdomains become depleted rapidly, resulting in a rapidly decreasing driving force for interphase mass transfer. Thus a steady-state plateau never develops. Of the values shown here, clearly $\lambda = 0.1$ (Figure 2b) is optimal in that it provides a steady-state release plateau with a rela-

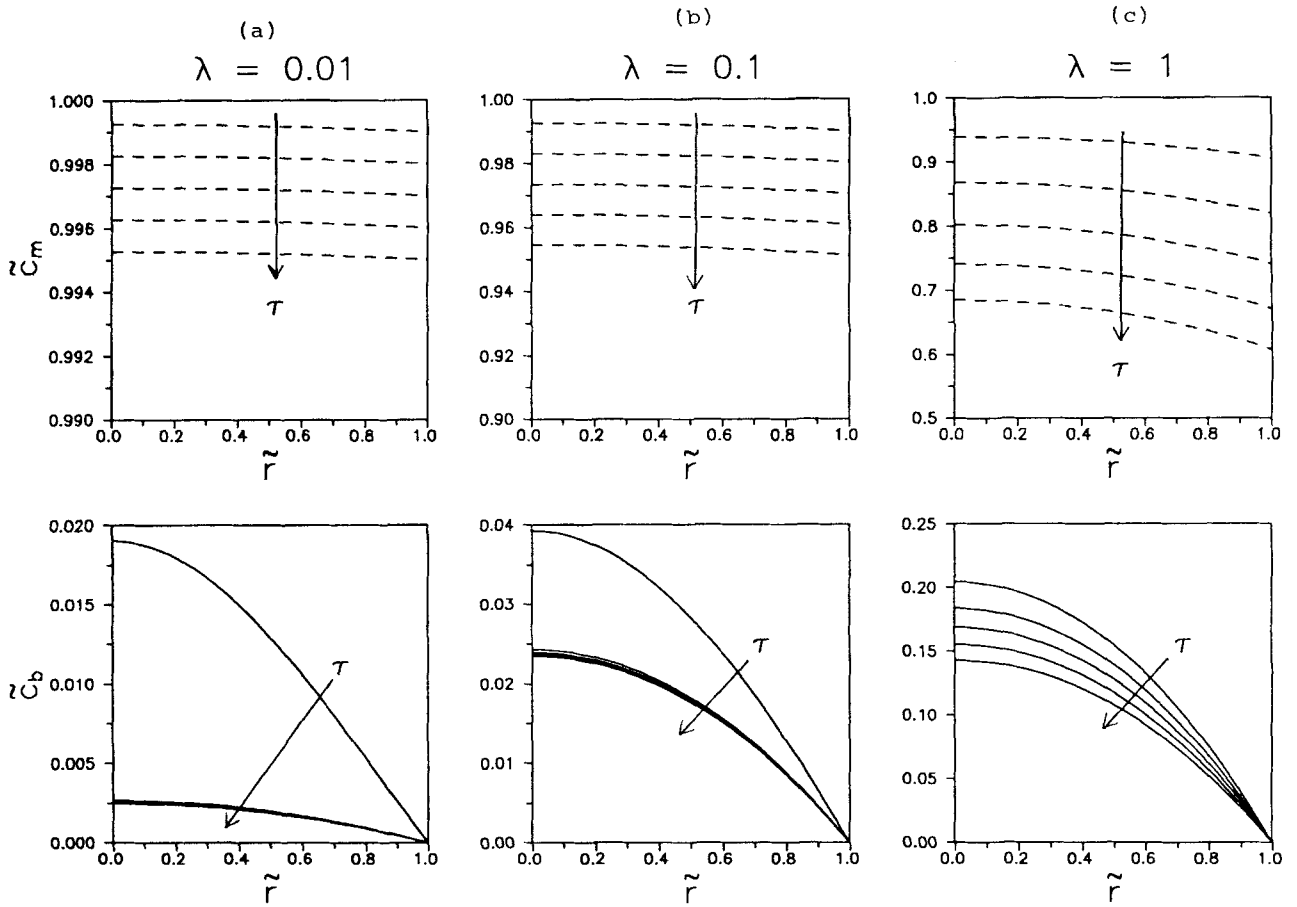

Figure 2. Radial concentration profiles in both phases of the device for $\kappa = 0.1$.

(a) $\lambda = 0.01$; (b) $\lambda = 0.1$; (c) $\lambda = 1.0$. $\Delta\tau = 1$ and $0 \le \tau \le 5$ for all plots.

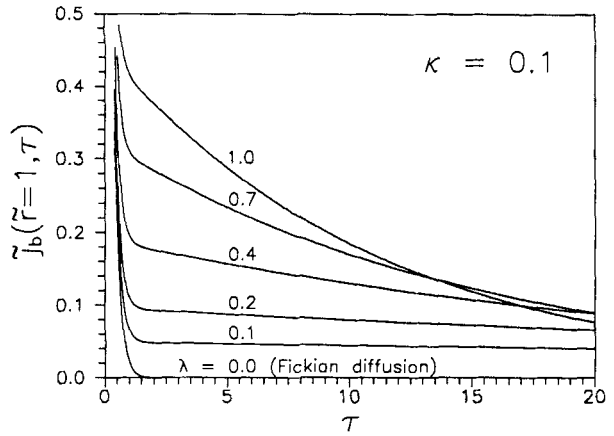

Figure 3. Dimensionless drug flux to the surroundings, $\kappa = 0.1$.

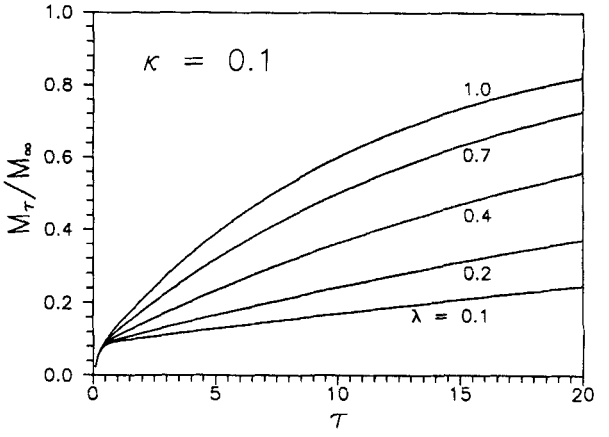

Figure 5. Cumulative solute released as a function of time, $\kappa = 0.1$.

tively high flux to the surroundings. Note that in the case where the second boundary condition is not satisfied, and the surface of the device is not perfectly washed of the drug at all times, there will be additional holdup in the bulk phase and the release will be attenuated further.

The effect of κ on the release profiles mirrors that of λ, as expected. Zero-order release can be sustained for longer periods as the volume fraction of microdomains, and hence the total drug loading in the domains, increases. When κ is high, we observe behavior approaching Fick's law diffusion right from the beginning of operation due to early depletion of the microdomains. On the other hand, as κ approaches zero the network structure approaches a single phase.

The dimensionless flux of drug to the surroundings is shown in Figure 3 for $\kappa = 0.1$ with varying λ. The flux is characterized by a brief initial steep drop followed by a plateau or near-plateau for low values of λ, or simply a more gradual decrease with no plateau for $\lambda > 0.4$. The magnitude of the steady-state flux for a given κ depends on λ. Figure 4 is a cross-plot showing the effect of κ on the flux at constant λ.

Figures 5 and 6 show the cumulative drug released from the device over time for constant κ with varying λ and for constant λ with varying κ, respectively. There is an initial high efflux of drug followed by a slower and in some cases steady release to the surroundings. In general the profiles deviate from linearity when more than ~ 50–60% of the drug has exited the device. As the microdomains become depleted of drug, the driving force for interphase mass transfer decreases. The bulk phase concentration begins to drop rapidly and a time-dependent release rate results.

Discussion

The effect of dispersed reservoirs on the release of drugs or other solutes from a network is to attenuate the depletion of the bulk phase during operation. With an appropriate pairing of solute and network properties, this can result in a near constant flux to the surroundings for a finite period, that is, zero-order release.

The dispersed-phase hydrogels that we have developed are an example of a system that can be described by this model. These gels form spontaneously in aqueous solutions containing hydrophobically modified water-soluble polymers. The hydrophobic side chains on the polymer self-assemble into micelle-like aggregates so as to minimize unfavorable interactions of the side chains with water. This has the effect of

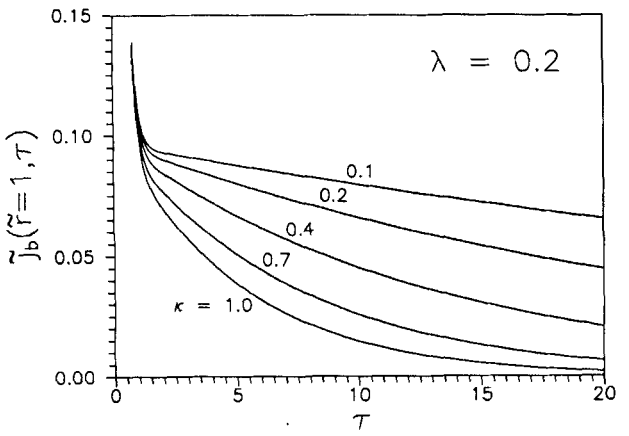

Figure 4. Dimensionless drug flux to the surroundings, $\lambda = 0.2$.

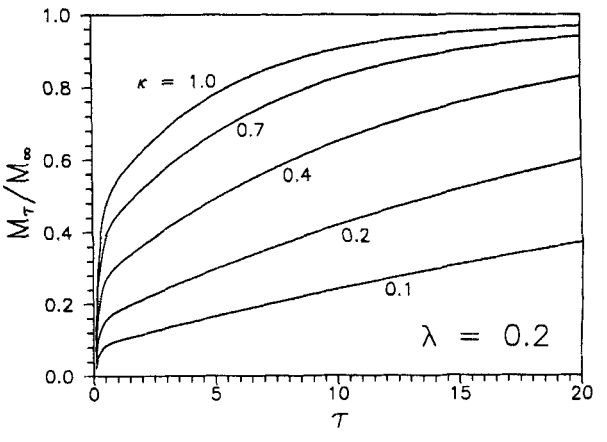

Figure 6. Cumulative solute released as a function of time, $\lambda = 0.2$.

bridging multiple polymer molecules, forming a viscoelastic water-swollen hydrogel with a hydrophobic dispersed phase. We can manipulate the aggregation number and composition of the microdomains by adjusting the composition of the solvent (Dualeh and Steiner, 1991). This permits control over both the relative solubility of the solute in the domains, α, and their geometry (hence h_b) and interfacial area, A_i. The total concentration of polymer in the gel governs the volume fraction of microdomains, ϕ (Varelas and Steiner, 1991). We have also learned (Wu et al., 1995) that the porosity of the interface, and hence h_i, is a function of the processing temperature of the gel. The bulk phase solubility, c^*, and diffusivity, D_b, of the drug can be assumed to be the same as in water (Haggerty et al., 1988). Finally, the microdomain radius, r_m, as well as h_i and α, will all depend on the chemical structure of the side chains on the polymer. Thus *we can manipulate all of the important structural parameters of our gels independently*, by varying either specific processing conditions or the structure of the starting polymer, to optimize the release characteristics for a particular drug.

The release profiles in Figure 4 can be used as design curves for controlled release devices made from dispersed-phase polymer gels. We start by specifying a drug compound, which constrains only D_b. We then specify the desired average release rate, an acceptable minimum release rate during operation (such as ≤ 90 percent of the average flux in the "plateau"), and a desired duration of sustained release. This determines the operating values for κ and λ. Then we select a polymer and identify processing conditions that will give the appropriate combination of α, A_i, h, and ϕ for that drug. If the appropriate combination cannot be obtained, a new polymer must be selected.

The results in Figure 3 demonstrate the importance of the interfacial mass-transfer resistance, h. It is possible that as the microdomains become depleted of drug the structure of the interface may change. Whether or not this occurs will depend on where in the microdomain the drug is solubilized and on the steric and electrostatic constraints the drug brings to bear on the other components of the domain. However, it is of course in our interest to maintain a constant interfacial resistance if we are to control the release rate from the device. One way to ensure this would be to swell the microdomains by incorporating a water-insoluble oil, thereby leaving the interface relatively unaffected as drug is depleted. Note that this model also applies to a dispersion of solute-loaded capsules whose structure would not be affected by depletion of the solute.

The results of this model may be applied to other systems characterized by a first-order release process occurring in tandem with bulk diffusion.

Acknowledgments

The authors wish to thank Prof. Charles Maldarelli of the City College of New York and Dr. Bret Berner of Ciba-Geigy Corporation for their suggestions and discussions relating to this work.

Notation

A_i = total bulk/microdomain interfacial area, m^2
c = total solute concentration in the gel, $kg \cdot m^{-3}$ gel
c^* = solute saturation concentration in bulk phase, $kg \cdot m^{-3}$ bulk
c_b = solute concentration in the bulk phase, $kg \cdot m^{-3}$ bulk
$\tilde{c}_b$ = dimensionless solute concentration in the bulk phase
c_m = solute concentration in the microdomains, $kg \cdot m^{-3}$ microdomains
$\tilde{c}_m$ = dimensionless solute concentration in the microdomains
D_b = solute diffusivity within the bulk phase, $m^2 \cdot s^{-1}$
D_{eff} = effective diffusivity in the gel, $m^2 \cdot s^{-1}$
h = overall mass-transfer coefficient at bulk/microdomain interface, $m \cdot s^{-1}$
h_b = mass-transfer coefficient of the stagnant boundary layer in the bulk phase, $m \cdot s^{-1}$
h_i = mass-transfer coefficient of the microdomain interface, $m \cdot s^{-1}$
j_b = solute flux, $kg \cdot m^{-2} \cdot s^{-1}$
$\tilde{j}_b$ = dimensionless solute flux
$M(s)$ = Laplace domain eigenvalue defined in Eqs. 14 and 15
M_τ = mass of solute released at time τ, kg
M_∞ = total mass of solute available for release, kg
$N(s_k^n)$ = function of nth quadratic roots defined in Eq. 18
r = radial position within delivery device, m
r_m = microdomain radius, m
$\tilde{r}$ = dimensionless radius of delivery device
R = external radius of delivery device, m
s = Laplace domain variable
s_k^n = nth quadratic roots (poles) defined in Eq. 18
t = time, s
V = total gel volume, m^3

Greek letters

α = solute partition coefficient, m^3 domain/m^3 bulk
κ = solute distribution coefficient, dimensionless
λ = Damköhler number, dimensionless
ξ_n = nth zero of the zero-order Bessel function of the first kind
τ = diffusion time, dimensionless
ϕ = volume fraction of microdomains, m^3 domain/m^3 total

Literature Cited

Baker, R. W. *Controlled Release of Biologically Active Agents*, Wiley, New York (1987).

Churchill, R. V., *Operational Mathematics*, 2nd ed., McGraw-Hill, New York (1958).

Cussler, E. L., *Diffusion: Mass Transfer in Fluid Systems*, Cambridge University Press, Cambridge, England, p. 186 (1984).

Dualeh, A. J., and C. A. Steiner, "Bulk and Microscopic Properties of Surfactant-Bridged Hydrogels Made from an Amphiphilic Graft Copolymer," *Macromolc*, **24**, 112 (1991).

Dualeh, A. J., and C. A. Steiner, "Structure and Properties of Surfactant-Bridged Viscoelastic Hydrogels," *Polyelectrolyte Gels: Properties, Preparation, and Applications, ACS Symp. Ser.*, R. S. Harland and R. K. Prud'homme, eds., Vol. 480, American Chemical Society, Washington, DC, p. 42 (1992).

Haggerty, L., J., Sugarman, and R. Prud'homme, "Diffusion of Polymers Through Polyacrylamide Gels," *Polym.*, **29**, 1058 (1988).

Rosner, D. E., *Transport Processes in Chemically Reacting Flow Systems*, Butterworths, Boston, p. 436 (1986).

Varelas, C. G., and C. A. Steiner, "Bulk and Microscopic Properties of Copolymer Networks in Mixed Aqueous Solvents," *J. Polym. Sci. B: Polym. Phys. Ed.*, **30**, 1233 (1991).

Varelas, C. G., D. G. Dixon, and C. A. Steiner, "Zero-Order Release from Biphasic Polymer Hydrogels," *J. Controlled Release*, in press (1995).

Wu, S.-Y., R. Varadaraj, and C. A. Steiner, "Effects of Temperature on the Structure of Two-Phase Hydrogels," *J. Phys. Chem.*, in press (1995).

Appendix: Inversion from the Laplace to the Time Domain

In order to obtain Eq. 18 from Eq. 17, we must perform inverse Laplace transformation, hence

$$\tilde{c}_b = \mathfrak{L}^{-1}\{\bar{c}_b\} = \mathfrak{L}^{-1}\left\{\frac{1}{s}\right\} - \mathfrak{L}^{-1}\left\{\frac{I_0[M(s)\tilde{r}]}{sI_0[M(s)]}\right\}. \quad \text{(A1)}$$

Inverse transformation of the first term is straightforward:

$$\mathfrak{L}^{-1}\left\{\frac{1}{s}\right\} = 1. \quad \text{(A2)}$$

For the second term we employ the theory of residues:

$$\mathfrak{L}^{-1}\left\{\frac{I_0[M(s)\tilde{r}]}{sI_0[M(s)]}\right\} = \sum_{n=1}^{\infty} \operatorname*{Res}_{s_n}\left(\frac{I_0[M(s)\tilde{r}]e^{s\tau}}{sI_0[M(s)]}\right) = \sum_{n=1}^{\infty} \lim_{s\to s_n} \frac{(s-s_n)I_0[M(s)\tilde{r}]e^{s\tau}}{sI_0[M(s)]} \quad \text{(A3)}$$

where s_n are the poles of the function in parentheses. By inspection, we see that the function has poles at $s = 0$ and at $I_0[M(s)] = 0$, or $M(s) = i\xi_n$, where $\xi_1, \xi_2, \ldots$ are the positive zeros of I_0. To find the nonzero (simple) poles, we simply solve the following quadratic equation

$$M(s) = \left[s + \frac{s\lambda}{s+\kappa\lambda}\right]^{1/2} = i\xi_n, \quad \text{(A4)}$$

which gives two roots corresponding to every positive zero ξ_n

$$s^n_{1,2} = \frac{-(\xi_n^2 + \lambda + \kappa\lambda) \pm \sqrt{(\xi_n^2 + \lambda + \kappa\lambda)^2 - 4\kappa\lambda\xi_n^2}}{2}. \quad \text{(A5)}$$

Hence, residues must be evaluated for each of the three poles:

$$\mathfrak{L}^{-1}\left\{\frac{I_0[M(s)\tilde{r}]}{sI_0[M(s)]}\right\} = \left(\operatorname*{Res}_0 + \sum_{n=1}^{\infty}\operatorname*{Res}_{s_1^n} + \sum_{n=1}^{\infty}\operatorname*{Res}_{s_2^n}\right)\left(\frac{I_0[M(s)\tilde{r}]e^{s\tau}}{sI_0[M(s)]}\right). \quad \text{(A6)}$$

Determination of the residue at $s = 0$ by Eq. A3 is straightforward, and is simply equal to one. For the simple poles, we employ the following formula:

$$\operatorname*{Res}_{s_n}\left(\frac{p(s)}{q(s)}\right) = \frac{p(s_n)e^{s_n\tau}}{q'(s_n)} \quad \text{(A7)}$$

where $p(s) = I_0[M(s)\tilde{r}c]$, and $q(s) = sI_0[M(s)]$. Hence, we obtain

$$\operatorname*{Res}_{s_1^n}\left(\frac{I_0[M(s)\tilde{r}]e^{s\tau}}{sI_0[M(s)]}\right) = \frac{I_0[M(s_1^n)\tilde{r}]e^{s_1^n\tau}}{s_1^n I_0'[M(s_1^n)]M'(s_1^n)} \quad \text{(A8)}$$

$$\operatorname*{Res}_{s_2^n}\left(\frac{I_0[M(s)\tilde{r}]e^{s\tau}}{sI_0[M(s)]}\right) = \frac{I_0[M(s_2^n)\tilde{r}]e^{s_2^n\tau}}{s_2^n I_0'[M(s_2^n)]M'(s_2^n)}. \quad \text{(A9)}$$

Recognizing the Bessel function identities

$$I_0(i\xi_n) = J_0(\xi_n) \quad \text{(A10)}$$

$$I_0'(i\xi_n) = I_1(i\xi_n) = iJ_1(\xi_n), \quad \text{(A11)}$$

and evaluating the derivative of $M(s)$

$$M'(s) = \frac{1}{2M(s)}\left[1 + \frac{\kappa\lambda^2}{(s+\kappa\lambda)^2}\right] = \frac{1}{2i\xi_n}\left[1 + \frac{\kappa\lambda^2}{(s+\kappa\lambda)^2}\right], \quad \text{(A12)}$$

we combine Eqs. A1, A2, A6, and A8 through A12 to obtain the solution

$$\tilde{c}_b(\tilde{r},\tau) = -\sum_{n=1}^{\infty}\frac{2\xi_n J_0(\xi_n\tilde{r})e^{s_1^n\tau}}{s_1^n J_1(\xi_n)N(s_1^n)} - \sum_{n=1}^{\infty}\frac{2\xi_n J_0(\xi_n\tilde{r})e^{s_2^n\tau}}{s_2^n J_1(\xi_n)N(s_2^n)} \quad \text{(A13)}$$

$$= -\sum_{k=1}^{2}\sum_{n=1}^{\infty}\frac{2\xi_n J_0(\xi_n\tilde{r})e^{s_k^n\tau}}{s_k^n J_1(\xi_n)N(s_k^n)} \quad \text{(18)}$$

where $N(s_k^n)$ is defined

$$N(s_k^n) = 1 + \frac{\kappa\lambda^2}{(s_k^n + \kappa\lambda)^2} \quad \text{(19)}$$

Manuscript received Oct. 20, 1993, and revision received Apr. 26, 1994.